NEOPLASIA
www.neoplasia.com

Volume 11 Number 2 February 2009 pp. 145–156 145

Enhanced Antitumorigenic Effects in Glioblastoma on Double Targeting of Pleiotrophin and Its Receptor ALK[1]

Marius Grzelinski*, Florian Steinberg*, Tobias Martens†, Frank Czubayko*, Katrin Lamszus† and Achim Aigner*

*Department of Pharmacology and Toxicology, Philipps-University School of Medicine, Marburg, Germany; †Department of Neurosurgery, University Medical Center Hamburg-Eppendorf, Hamburg, Germany

Abstract

In adults, glioblastomas are the most lethal and most frequent malignant brain tumors, and the poor prognosis despite aggressive treatment indicates the need to establish novel targets for molecular intervention. The secreted growth factor pleiotrophin (PTN, HB-GAM, HBNF, OSF-1) shows mitogenic, chemotactic, and transforming activity. Whereas PTN expression is tightly regulated during embryogenesis and is very limited in normal adult tissues, a marked PTN up-regulation is seen in tumors including glioblastomas. Likewise, the PTN receptor anaplastic lymphoma kinase (ALK) has been shown previously to be upregulated and functionally relevant in glioblastoma. In this study, we explore the antitumorigenic effects of the simultaneous ribozyme-mediated knockdown of both receptor and ligand. Various glioblastoma cell lines are analyzed for PTN and ALK expression. Beyond the individual efficacies of several specific ribozymes against PTN or ALK, respectively, antiproliferative and proapoptotic effects of a single gene targeting approach are strongly enhanced on double knockdown of both genes *in vitro*. More importantly, this results in the abolishment of tumor growth in an *in vivo* subcutaneous tumor xenograft model. Finally, the analysis of various downstream signaling pathways by antibody arrays reveals a distinct pattern of changes in the activation of signal transduction molecules on PTN/ALK double knockdown. Beyond the already known ones, it identifies additional pathways relevant for PTN/ALK signaling. We conclude that double targeting of PTN and ALK leads to enhanced antitumorigenic effects over single knockdown approaches, which offers novel therapeutic options owing to increased efficacy also after prolonged knockdown.

Neoplasia (2009) 11, 145–156

Introduction

Glioblastomas, which can progress from lower grade gliomas or arise *de novo*, are the most frequent and lethal brain tumors in adults. Because nearly all patients die within 12 months despite aggressive treatment including surgery, chemotherapy and radiation [1], the functional analysis of molecules and pathways relevant in glioblastoma pathogenesis is of major importance to developing novel therapeutic strategies based on targeted molecular therapies.

The secreted growth factor pleiotrophin (PTN), also called heparin-binding growth-associated molecule (HB-GAM), heparin affin regulatory peptide (HARP), heparin-binding growth factor 8, heparin-binding neurotrophic factor (HBNF), or osteoblast-specific protein-1 (OSF-1), is a 15.3-kDa developmentally regulated cytokine, which shows very limited expression in normal adult tissues, but is markedly upregulated in various primary human tumors and tumor cell lines [2–10]. In particular, cDNA arrays [11] as well as ELISA and immunohistochemistry [12], have shown increased PTN expression in glioblastomas compared to normal human brain tissue, and all WHO III and IV grade gliomas are positive for PTN [13]. Concomitantly, PTN exerts oncogenic potential and acts as a mitogenic, chemotactic, and angiogenic factor in various cells including tumor cell lines and tumors [5,9,14–18].

Abbreviations: PTN, pleiotrophin; ALK, anaplastic lymphoma kinase; MK, midkine

Address all correspondence to: Dr. Achim Aigner, Department of Pharmacology and Toxicology, Philipps-University Marburg, Karl-v.-Frisch-Strasse 1, D – 35033 Marburg, Germany. E-mail: aigner@staff.uni-marburg.de

[1]This work was supported by a grant (AI 24/5-1) from the Deutsche Forschungsgemeinschaft (DFG) to A.A. and by a fellowship from the FAZIT foundation to M.G.
Received 27 August 2008; Revised 3 November 2008; Accepted 5 November 2008

DOI 10.1593/neo.81040

In particular, ribozyme- or antisense- or RNA interference (RNAi)–mediated gene targeting of PTN has been demonstrated to suppress the proliferative and tumorigenic effects of PTN with concomitant reduction of tumor growth, tumor angiogenesis, and metastatic spread in various tumor entities [5,19,20] including glioblastoma [21,22].

Previously, PTN has been shown to signal through anaplastic lymphoma kinase (ALK) [23–25], a transmembrane tyrosine kinase receptor, which was first identified as a constitutively active, oncogenic chimeric nucleophosmin–ALK fusion protein resulting from the (2;5)(p23;q35) chromosomal translocation in anaplastic large cell lymphomas [26–28] (see [29] for review). By phage display, PTN was demonstrated to bind to the extracellular domain of ALK, thus mediating growth stimulatory [24] and antiapoptotic effects [23]. ALK is overexpressed in glioblastoma compared to normal brain, and ribozyme-mediated targeting of ALK led to reduced tumor growth of glioblastoma xenografts in athymic nude mice and increased apoptosis in the tumors [25]. Additionally, it was shown that PTN interacts with the receptor-type protein tyrosine phosphatase β/ζ (RPTPβ/ζ) [30], which is also overexpressed in glioblastoma [11], and that ALK can be activated through the PTN/RPTPβ/ζ pathway, thus introducing a unique "alternative mechanism of tyrosine kinase receptor activation" [31]. This indicates that ALK is involved in all PTN-mediated signal transduction pathways. The ligand PTN [21] as well as the receptors ALK [25] and RPTPβ/ζ [32] have been demonstrated to be relevant in glioblastoma growth, and targeting of each of these gene products exerts antitumorigenic effects.

In this study, we selected ALK as a central player in PTN-mediated signal transduction pathways, and PTN as target molecules in a ribozyme-based approach of gene knockdown. We show that the combination of both ligand + receptor knockdown leads to increased antitumor effects. Antiproliferative and proapoptotic effects of single knockdowns were strongly enhanced on double knockdown of both proteins *in vitro*, and even the abolishment of tumor growth was observed in an *in vivo* subcutaneous (SC) tumor xenograft model. Finally, the antibody array–based analysis of various downstream signaling pathways reveals a distinct pattern of changes in the activation of signal transduction molecules on PTN/ALK double targeting and, beyond the already known ones, identifies additional pathways as relevant for PTN/ALK signaling.

Materials and Methods

Cell Lines, Ribozyme Constructs, and Stable Transfection

The glioblastoma cell lines G122, U118, U87, and T98G were obtained from the American Type Culture Collection (ATCC, Manassas, VA), and the cell line G55T2 was established as described previously [33]. All cell lines were cultivated under standard conditions (37°C, 5% CO_2) in Iscove's modified Dulbecco's medium (PAA Laboratories, Cölbe, Germany) supplemented with 10% fetal calf serum (FCS) unless indicated otherwise.

Ribozyme expression vectors were constructed by annealing synthetic sense and antisense oligonucleotides containing the hammerhead ribozyme sequence flanked by PTN- or ALK-specific recognition sequences as well as a *Hind*III and a *Not*I site, and cloning them as described previously [21,25] into the pRc/CMV vector (Invitrogen, Carlsbad, CA). Ribozyme sequences were as follows:

PTN 66: 5′-cauucauuuuaagcaggauugccugaguaguccauacuggc-3′,
PTN 261: 5′-cuacauucuaaagcaggauugccugaguagucgggacguug-3′,
ALK 1-3: 5′-agcttggagctatctgatgagtccgttaggacgaaaccagtccgc-3′,
ALK 3-2: 5′-agctttccactgcactgatgagtccgttaggacgaaacaagctgc-3′,
ALK 12-1: 5′-agcttgccgtaattctgatgagtccgttaggacgagaacattccgc-3′.

Stable transfections were performed in six-well plates with 100,000 cells per well and 3 μg of the ribozyme expression vector, or the empty vector as negative control, using jetPEI as described by the manufacturer (Polyplus, Illkirch, France). Selection for stable integrants started 48 hours after transfection by the addition of 1000 μg/ml G418 (PAA Laboratories) for 3 weeks. For double targeting, stable cell lines were again cotransfected with 3 μg of the second ribozyme expression vector + 0.3 μg pcDNA Hygro+ vector (Invitrogen), and 400 μg/ml hygromycin was used for the selection for stable integrants.

RNA Preparation and Quantitative Reverse Transcription–Polymerase Chain Reaction

Total RNA from tumor cells was isolated using the Tri reagent (PEQLAB, Erlangen, Germany) according to the manufacturer's protocol. Reverse transcription (RT) was performed using the RevertAid H Minus First Strand cDNA Synthesis Kit from Fermentas (St. Leon-Rot, Germany) as follows: 1 μg total RNA was diluted in 12 μl of diethylpyrocarbonate-treated water and 1 μl of random hexames primer (0.2 μg/μl) was added, the mixture was incubated at 70°C for 5 minutes and chilled on ice before adding 4 μl of 5× reaction buffer, 0.5 μl RNAse inhibitor (20 U/μl), and 2 μl of 10 mM dNTP mix. After incubating at 25°C for 5 minutes, 1 μl of reverse transcriptase (200 U/μl) was added, and the mixture was incubated for 10 minutes under the same conditions and for 60 minutes at 42°C, before stopping the reaction by heating at 70°C for 10 minutes and chilling on ice. Quantitative polymerase chain reaction (PCR) was performed in a LightCycler from Roche (Penzberg, Germany) using the QuantiTect SYBR Green PCR kit (Qiagen, Hilden, Germany) according to the manufacturer's protocol with 4 μl of cDNA (diluted 1:100), 5 μl of SYBR Green Master Mix, and 1 μl of primers (5 μM) specific for PTN, ALK, RPTPβ/ζ, MK, or the ribozyme expression vector (SP6 and T7 primers). To normalize for equal loading, all samples were run in parallel with actin primers. A preincubation for 15 minutes at 95°C was followed by 55 amplification cycles: 10 seconds at 95°C, 10 seconds at 55°C, and 10 seconds at 72°C. The melting curve for PCR product analysis was determined by rapid cooling down from 95 to 65°C and incubating at 65°C for 15 seconds before heating to 95°C.

PTN ELISA

Conditioned tissue culture medium was assayed for PTN protein essentially as described previously [3]. Briefly, 100 μl per well of a mouse anti-PTN monoclonal antibody (4B7), diluted to 1 μg/ml in Tris-buffered saline (TBS), was incubated in covered 96-well ELISA plates (Life Technologies, Karlsruhe, Germany) at 4°C overnight. After washing three times with TBS/0.5% Tween 20 (TBST), wells were blocked with 200 μl of TBST/1% BSA for 2 hours, washed again, and loaded with 100 μl of sample per well diluted 1:1 in TBST for 1 hour. After washing, 100 μl per well of biotinylated affinity-purified goat anti–(human PTN) detection antibody (R&D Systems, Wiesbaden, Germany) was added at a concentration of 500 ng/ml and was incubated for 1 hour, and wells were washed again and incubated with 100 μl per well of Streptavidin-AP conjugate (Roche Diagnostics, Mannheim, Germany; 1:5000 in TBST) for 1 hour. After a final wash, the signal was revealed with 100 μl per well of *p*-nitrophenyl

phosphate substrate solution for 2 hours, and absorbance was measured in an ELISA reader at 405 nm. Recombinant human PTN (R&D Systems) served as the standard.

In Vitro *Proliferation Assays and* In Vitro *Scratch Assay*

Anchorage-dependent proliferation was assessed essentially as described previously [34]. Briefly, cells were plated in quadruplicates into 96 well plates at, dependent on the cell line, 500 to 1000 cells per well and cultivated in IMDM/10% FCS in a humidified incubator under standard conditions. Numbers of viable cells were assessed using a colorimetric assay according to the manufacturer's protocol (Cell Proliferation Reagent WST-1; Roche Molecular Biochemicals, Mannheim, Germany).

To determine anchorage-independent proliferation leading to colony formation, soft agar assays were carried out as described previously [35]. Briefly, 20,000 cells in 0.8 ml of 0.35% agarose were layered on top of 1 ml of a solidified 0.6% agar layer in a 35-mm dish. Growth media with 10% FCS were included in both layers. Colonies more than 50 μm in diameter were counted, dependent on the proliferation rate of the cell lines, after 2 to 5 weeks of incubation by at least two independent investigators blinded to the study.

In vitro scratch assays were performed essentially as described previously [36]. Briefly, cells were plated in wells, and after 4 days, scratches were created by scraping with a 200-μl pipette tip. Cell motility was determined microscopically at the time points 0 and 6 hours by photographing the gaps using a bright field microscope at low magnification and measuring changes in the gap width.

Apoptosis Assay

To test for *in vitro* apoptosis, the Caspase-Glo 3/7 assay (Promega, Madison, WI) was performed according to the manufacturer's protocol. Briefly, 4000 cells per well were plated in 96-well plates and were cultivated for 3.5 days. A total of 100 μl of Caspase-Glo 3/7 substrate, reconstituted in buffer, was added per well, and luminescence was measured after 4 hours using a Fluostar Optima reader (BMG Labtec, Jena, Germany). To normalize for differences in cell densities, a WST-1 assay was performed in parallel on the same plate, and the results of caspase activity, determined in five wells, were adjusted to cell numbers of the different cell lines.

Tumor Growth in Nude Mice

For the determination of *in vivo* tumor growth, 3×10^6 glioblastoma cells in 150 μl of PBS were injected SC into both flanks of athymic nude mice (*FoxN1 nu/nu*). When solid tumors became visible after 6 days, tumor sizes were determined every 2 to 3 days from the product of the perpendicular diameters of the tumors for a period of ~2.5 to 10 weeks, dependent on the cell line as indicated in the figure. Intracranial experiments were performed as described previously [32]. Briefly, mice were anesthetized by i.p. injection of ketamine and xylazine (100 and 5 mg/kg bodyweight, respectively) and a burr hole was drilled into the skull 3.5 mm lateral to the bregma. A total of 5 μl of a U87 cell suspension adjusted to a concentration of 10^5 cells/μl containing 0.8% methylcellulose were slowly injected for 5 minutes into the caudate/putamen, using a 30-G needle attached to a 25-μl Hamilton syringe. All animals were killed after 21 days when some of the mice started to develop symptoms (weight loss). Brains were embedded in paraffin, and serial 5-μm sections were stained with hematoxylin/eosin. The maximum cross-sectional areas of the glioblastoma xenografts were determined by computer-assisted image analysis using Leica IM50 software (Leica, Hamburg, Germany), and tumor volumes were estimated by the following formula: volume = (square root of maximal tumor cross-sectional area)^3.

Phospho-MAP Kinase Antibody Array Kit

The activity of a panel of mitogen-activated protein kinases (MAPKs) and other serine/threonine kinases was assessed through the determination of their relative level of phosphorylation using the Proteome Profiler Array (R&D Systems) according to the manufacturer's instructions. Briefly, stable double knockout cells and control cells were seeded at 50% confluency in wells of a six-well plate, grown for 2 days, and then lysed at 1×10^7 cells/ml in lysis buffer for 30 minutes at 4°C. After centrifuging at 14,000*g* for 5 minutes, the protein concentration of the supernatant was determined, and 250 μl of lysate, equivalent to 120 μg of protein, of each sample was diluted in 1.25 ml of Array Buffer 1. Arrays were preincubated in 1.5 ml of Array Buffer 1 for 1 hour before incubating the arrays in the sample dilution at 4°C overnight, 3 × 10 minutes washing in 20 ml of wash buffer, incubating in the detection antibody cocktail (1:100 in 1× Array Buffer 1), washing, and incubating in a Streptavidin-HRP solution (1:2000). After washing again, signals were developed by incubating in SuperSignal ECL solution (Thermo Fisher Scientific, Rockford, IL), and chemiluminescence was visualized by film exposure (Hyperfilm ECL; GE Healthcare, Munich, Germany) for various periods (10 seconds to 20 minutes) to analyze very strong as well as very weak spots. Signals were scanned and quantitated using ImageJ (National Institutes of Health, Bethesda, MD).

Data Analysis

For statistical analysis, one-way analysis of variance/Tukey posttests and two-way analysis of variance/Bonferroni posttests were used ($^*P < .05$, $^{**}P < .01$, $^{***}P < .001$).

Results

Expression of PTN, ALK, RPTPβ/ζ, and MK in Glioblastoma Cell Lines

Various glioblastoma cell lines were assessed by quantitative reverse transcription–polymerase chain reaction (RT-PCR) and ELISA for PTN and ALK expression with major differences being observed. More specifically, ALK expression was strong in G122 and U87 cells and weak or absent in G55T2 and T98G cells, but by far the highest *ALK* mRNA levels were observed in U118 cells (Figure 1*A*). Interestingly, the opposite was true for PTN expression, which, in U118 cells, was very low on the mRNA level and below the limit of detection on the protein level, respectively. In contrast, strong PTN expression was observed in G122, T98G, and U87 cells, with mRNA levels correlating very well with protein levels (Figure 1, *B* and *C*). On the basis of these data, G122 and U87 cells were selected for further experiments, which showed the best combination of strong PTN expression and ALK expression. Midkine (MK) is a protein related to PTN, which also signals through ALK and is also involved in tumorigenesis [37,38]. In G122, U87, and U118 cells, quantitative RT-PCR for MK revealed only weak MK expression, as opposed to G55T2 and T98G (Figure 1*D*). Finally, RPTPβ/ζ expression was rather low (U118, G55T2, U87MG) or almost absent (T98G) in

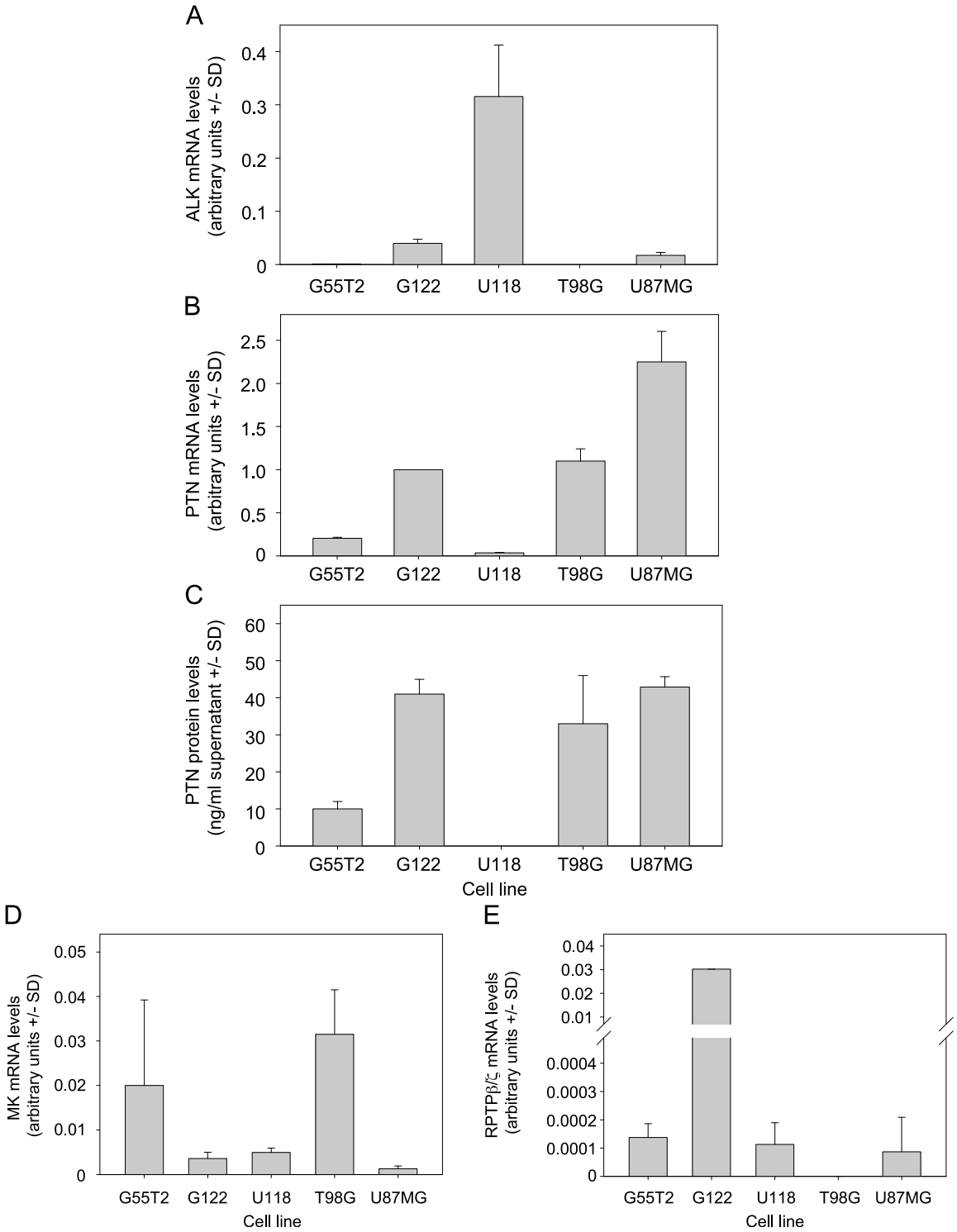

Figure 1. Expression of ALK, PTN, MK, and RPTPβ/ζ in various glioblastoma cell lines. Levels of (A) *ALK* mRNA, (B) *PTN* mRNA, (C) PTN protein in conditioned medium, (D) *MK* mRNA, (E) *RPTPβ/ζ* mRNA are shown.

glioblastoma cell lines, with the exception of G122, which showed very high RPTPβ/ζ levels (Figure 1*E*).

Establishment and Analysis of Stable PTN and ALK Knockdown

Expression vectors encoding ribozymes targeting PTN (Rz66, Rz261) or ALK (Rz1-3, Rz3-2, Rz12-1) were transfected and stably integrated into G122 and U87 cells. Reverse transcription–PCR using primers specific for the ribozyme expression vectors showed bands at the expected size (~100 bp, with the PTN Rz PCR product as predicted being slightly higher than the ALK Rz) in the stably transfected cells but not in the untransfected wild type cells, indicating the stable integration of the ribozymes (Figure 2*A*).

The analysis of *ALK* mRNA levels in G122 cells revealed a moderate yet statistically significant knockdown efficacy between 20% (Rz1-3) and 40% (Rz12-1) whereas on transfection of the empty

vector, *ALK* remained unchanged compared to wild type cells (Figure 2*B*). Considerably more pronounced targeting efficacies were observed in U87 cells with 85% to 90% ALK knockdown, with no significant differences between the three ribozymes (Figure 2*C*, *left*). Stable transfection with the PTN Rz expression vectors had no effect on ALK expression levels (data not shown) but resulted in the downregulation of PTN expression in G122 and in U87 cells with, again, the effect being less pronounced in G122 compared to that in U87 cells. More specifically, in G122 cells, a 25% (Rz66) to 50% (Rz261) knockdown was achieved on mRNA level (Figure 3*A*), whereas U87 cells showed a >70% reduction in *PTN* mRNA levels, which was again independent of the ribozyme (Figure 3*C*, *left*). PTN ELISA measurements of the conditioned medium also revealed that decreased mRNA levels were paralleled by reduced secretion of PTN protein (Figure 3*B*), indicating that mRNA reduction correlates well with decreased PTN protein expression. No changes in PTN levels were observed on stable ALK targeting (data not shown).

Subsequently, double knockdowns were performed in stable ribozyme-expressing U87 and G122 cells by stably transfecting the second ribozyme expression vector. Analysis of *ALK* (Figure 2*C*) and *PTN* (Figure 3*C*) mRNA levels revealed that knockdown efficacies of each individual ribozyme remained essentially unchanged on the introduction of the second ribozyme (Figures 2*C* and 3*C*, *right panels*; data not shown).

Enhanced Antiproliferative Effects on Double Knockdown of PTN and ALK

Stable reduction of ALK or PTN in U87 cells resulted in a significantly decreased anchorage-dependent proliferation (Figure 4, *A* and *B*), which was comparable for both gene products. Notably, however, double knockdown of both PTN and ALK markedly enhanced the antiproliferative effects (Figure 4*C*) with almost an abolishment of cell proliferation in the case of the most efficient ribozyme combination, Rz ALK 3-2/PTN 261 (compare Figures 2*C* and 3*C*). Likewise, stable targeting of both PTN and ALK led to increased antiproliferative effects in G122 cells compared to single knockdown (Figure 4*E*).

Soft agar assays rely on anchorage-independent cell proliferation and thus resemble more closely the *in vivo* situation. The assessment of colony formation of U87 cells stably transfected with one ribozyme expression vector revealed decreased proliferation. This was particularly true for ribozymes ALK 3-2 or PTN 261 (Figure 4*D*, *left and center panels*), which, in combination, had shown to be most efficient in the reduction of anchorage-dependent growth (compare Figure 4*C*). On double knockdown of both PTN and ALK, a markedly reduced

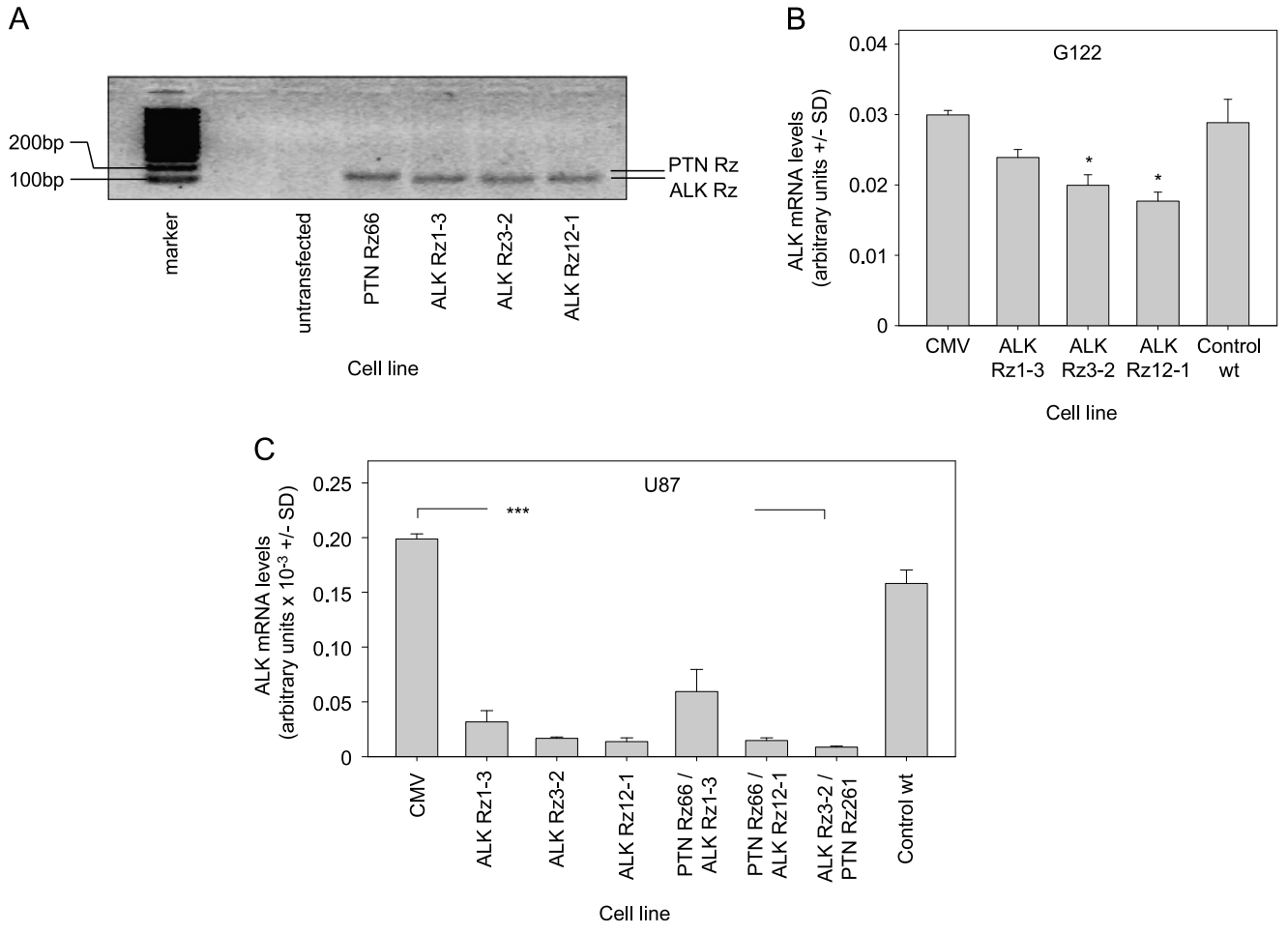

Figure 2. Ribozyme-mediated knockdown of ALK. (A) Expression of ribozymes in stably transfected cells as determined by PCR. Constitutive expression of ALK ribozymes Rz1-3, Rz3-2, or Rz12-1 leads to a moderate reduction of *ALK* mRNA levels in G122 (B) and to a profound *ALK* mRNA knockdown in U87 cells (C). Targeting efficacies remain unchanged on double knockdown of PTN and ALK (C, right panel). $*P < .05$, $***P < .001$ compared with vector control.

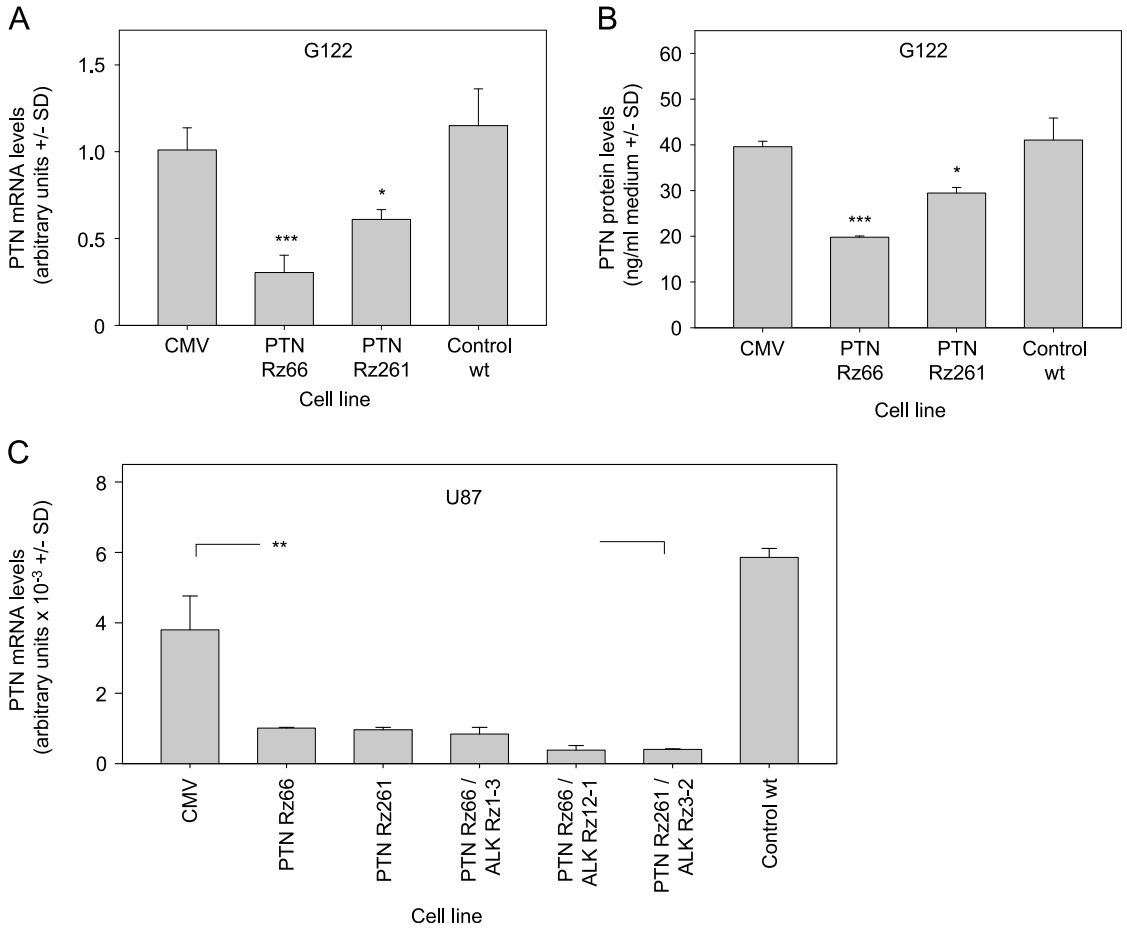

Figure 3. Ribozyme-mediated knockdown of PTN. Constitutive expression of PTN ribozymes Rz66 or Rz261 leads to the reduction of *PTN* mRNA levels in G122 cells (A), which translates into reduced PTN protein levels in the conditioned media (B). Strong *PTN* mRNA knockdown is observed in U87 cells (C). Targeting efficacies remain unchanged on double knockdown of PTN and ALK (C, right panel). $^{*}P < .05$, $^{**}P < .01$, $^{***}P < .001$ compared with vector control.

colony formation was observed in all ribozyme combinations analyzed, indicating additive antiproliferative effects over the single knockdown. In agreement with the data on the anchorage-dependent proliferation on double knockdown, the combination of ribozymes ALK 3-2 and PTN 261 resulted again in the almost complete abolishment of tumor cell proliferation (Figure 4*D*, *right panel*).

To further study cellular effects on PTN/ALK double knockdown, apoptosis and cellular migration were determined in selected cell lines. Caspases-3 and -7 play key effector roles in apoptosis, and their activities were measured in a luminescent assay. In stably ALK ribozyme– or PTN ribozyme–transfected cells, a ~1.5-fold increase in apoptosis was observed. More strikingly, however, on double knockdown of PTN and ALK, an almost three-fold higher caspase-3/7 activity was determined (Figure 4*F*). Likewise, differences were observed regarding cellular migration as determined by an *in vitro* scratch assay. Whereas 6 hours after scraping a ~20% reduction in scratch width was determined in the case of control cells, no cellular migration was observed in double knockdown cells (Figure 4*G*).

Double Knockdown of PTN and ALK Abrogates SC Tumor Growth

To test the antitumorigenic effects of the parallel targeting of PTN and ALK more rigorously, an *in vivo* subcutaneous tumor xenograft model was used. Poor proliferation of U87 Rz3-2/261 cells, however, prevented the generation of cell numbers sufficiently high for *in vivo* experiments, and so this cell line had to be excluded, and the double knockdown cell lines U87 Rz66/1-3 and Rz66/12-1 were selected instead. Also, reduced tumor growth on single targeting of PTN or ALK had already been reported previously [21,25] and was thus not included again in this experiment. Wild type or empty vector–transfected U87 cells rapidly grew tumors, which were accurately measurable after 6 days. For ethical reasons, the experiment was terminated in these groups after 16 to 20 days owing to the formation of very large tumors. In contrast, tumor growth was markedly reduced in cells stably transfected with ribozymes PTN 66/ALK 1-3 with an onset of tumor mass expansion only after day 20 and thus, after the experiment, had already been terminated in the control groups. Most strikingly, however, double transfection of U87 cells with ribozymes PTN 66 and ALK 12-1 completely inhibited tumor growth for more than a 60-day monitoring period (Figure 5).

Activity of Downstream Signal Transduction Pathways

Finally, the double knockdown cell line U87 Rz ALK 12-1/PTN 66, which also showed reduced tumor growth by >50% compared to untargeted control cells after stereotactical engraftment of the

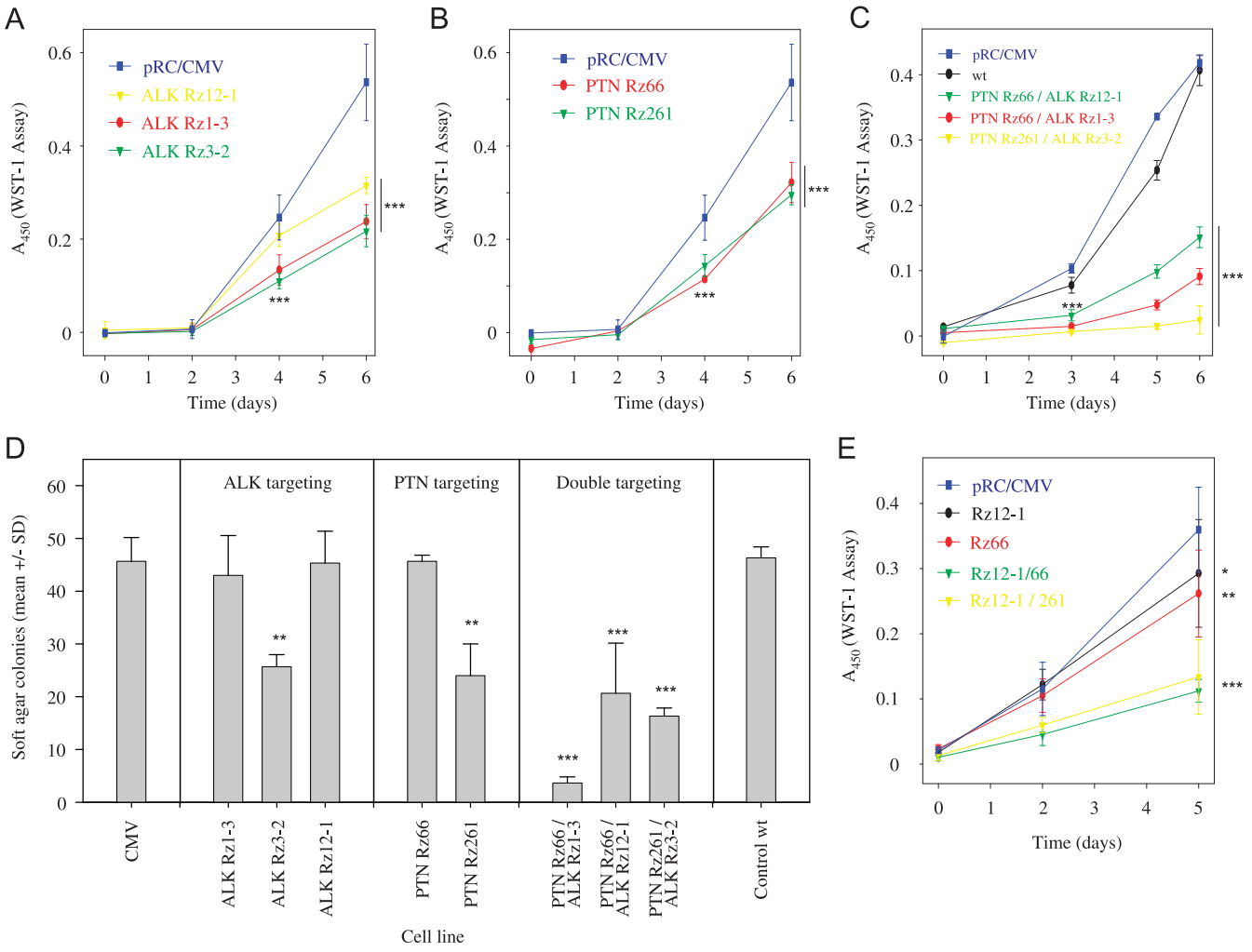

Figure 4. Antiproliferative effects of ribozyme-mediated knockdown of ALK (A) or PTN (B) in U87 cells. Double knockdown of PTN and ALK leads to a further reduction in U87 (C) and in G122 cell proliferation (E). Soft agar assays monitoring anchorage-independent cell growth of U87 cells confirm the enhanced antiproliferative effects on double knockdown (D). Caspase-3/-7 assays indicate increased apoptosis on single gene targeting of PTN or ALK and, more profoundly, in double knockdown cells (F). A scratch assay also reveals the inhibition of cell migration on PTN/ALK double knockdown as determined by the fold change in scratch width 6 hours after scraping (G, left; see right panel for representative examples). *$P < .05$, **$P < .01$, ***$P < .001$ compared with vector control.

cells into the caudate-putamen of nude mice (Figure 6*C*), was further analyzed about changes in downstream signal transduction pathways.

Using a phospho-specific antibody array, changes in the phosphorylation status of important regulators of signal transduction were analyzed after PTN/ALK double knockdown, including all three major families of MAPKs, the extracellular signal–regulated kinases (ERK1/2), c-Jun N-terminal kinases (JNK1-3), the different p38 isoforms α, β, δ, and γ, as well as the serine/threonine kinases Akt1, 2, 3, the glycogen synthase kinase GSK-3, and p70 S6 kinase (Figure 6*A*). Arrays were incubated in parallel with lysates from the double knockdown cell line U87 Rz ALK 12-1/PTN 66 and from untargeted control cells, and arrays were exposed to films for different periods not only to avoid film saturation when quantifying strong signals but also to detect very weak signals (see Figure 6*B* for one representative example). The comparison revealed that, on PTN/ALK double targeting, phosphorylation of HSP27, ribosomal kinase 2 (RSK2), and Akt3 dropped to levels below the level of detection even after a very long exposure to film. Essentially, no changes were observed in JNK and ERK phosphorylation, and changes in akt were limited to Akt3. In contrast, increased phosphorylation on PTN/ALK double knockdown was observed for RSK1, all members of the p38 family, GSK-3α, and GSK-3β, as well as for p70 S6 kinase (Figure 6*A*). Taken together, this indicates a rather complex pattern of changes in various signal transduction pathways.

Discussion

The growth factor PTN as well as both receptors involved in PTN signaling, ALK and RPTPβ/ζ, have been shown individually to be rate-limiting for glioblastoma growth and thus to play a pivotal role in this highly malignant tumor [21,25,32]. Owing to the genetic instability of tumor cells, which may lead to autocrine counterregulations and the probably limited efficacy of any targeting strategy, however, a single knockdown or inhibition may not be sufficient in a therapeutic setting, and the parallel inhibition of more than one gene involved in a given signal transduction pathway may be

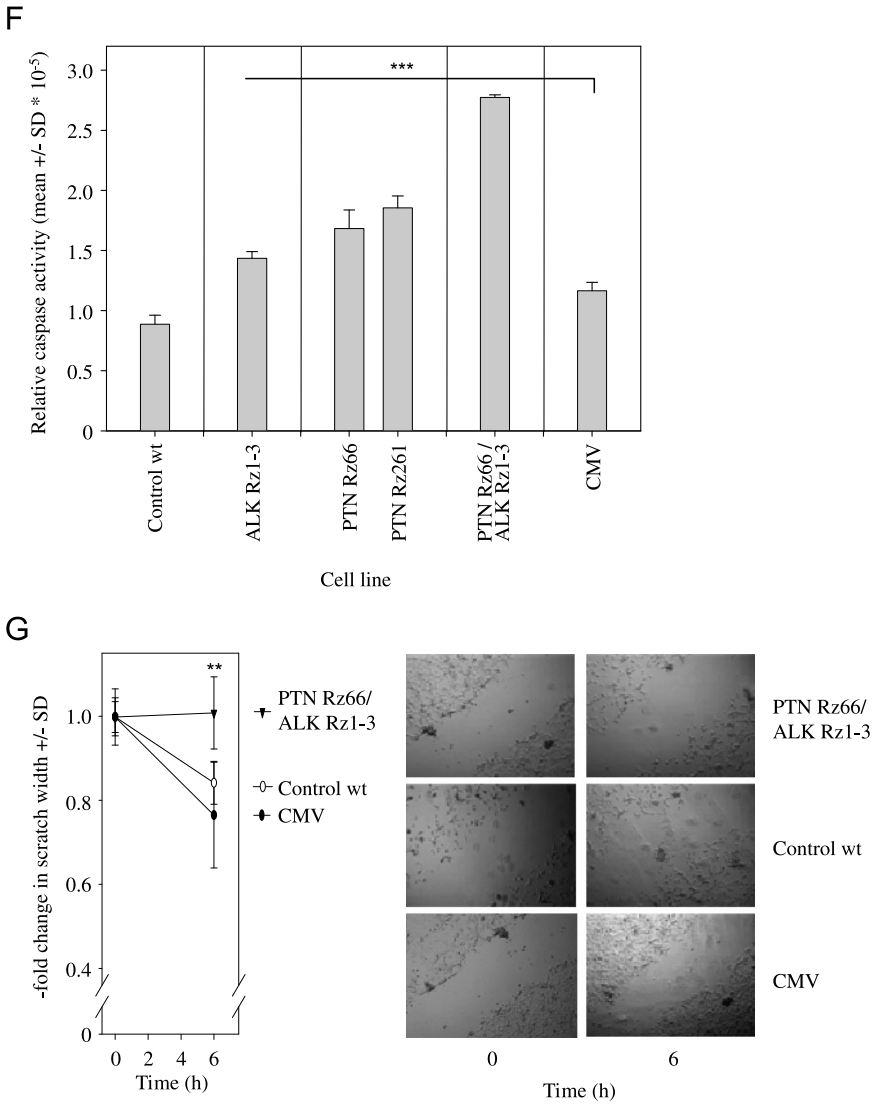

Figure 4. (*continued*)

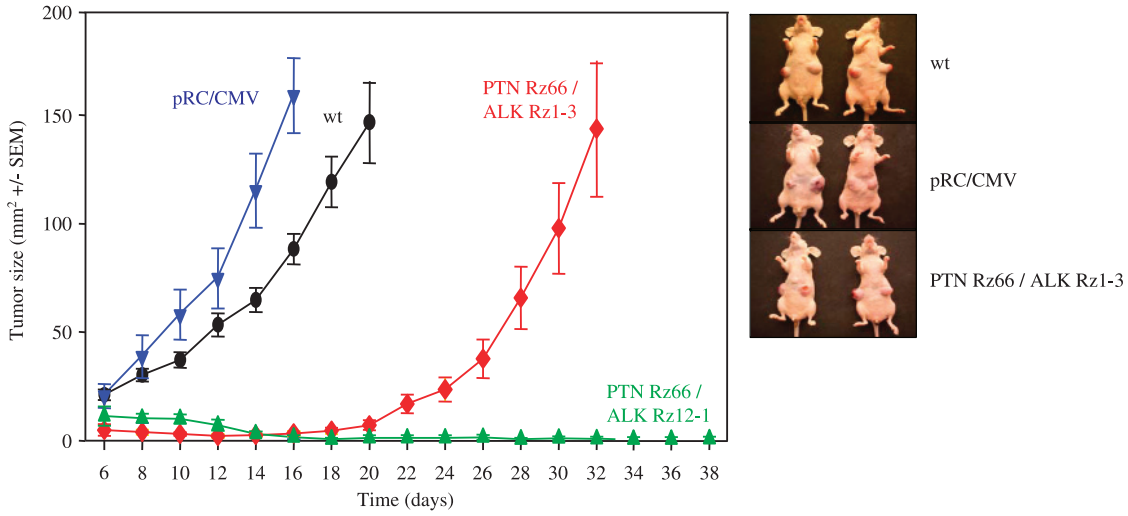

Figure 5. Abrogation of SC U87 tumor xenograft growth on PTN/ALK double knockdown using ribozymes PTN Rz66 and ALK Rz12-1. Right panel: Representative tumor-bearing mice at the time points of termination of the experiment as indicated in the growth curves.

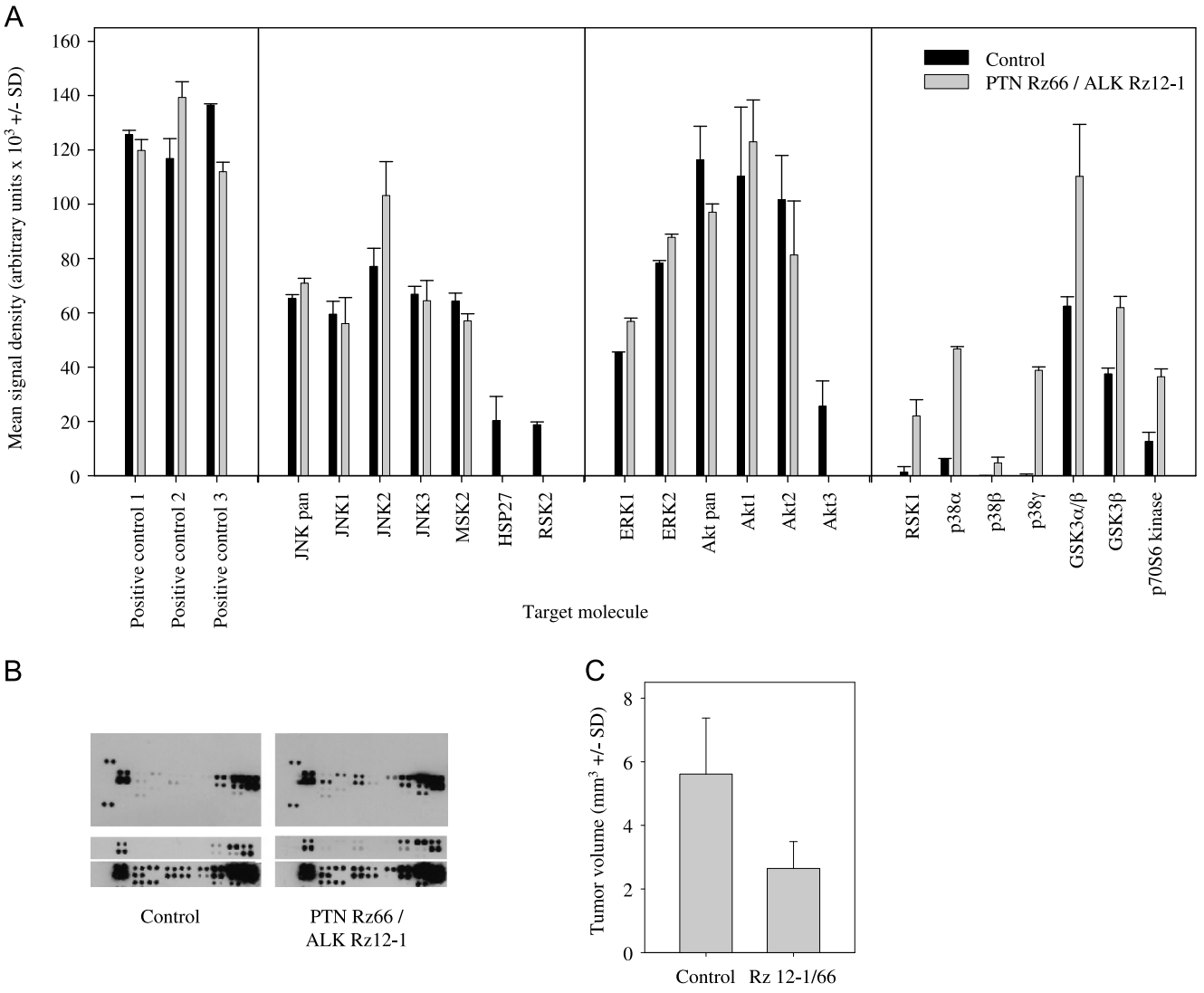

Figure 6. Antibody array data to assess the activity of downstream signal transduction pathways. (A) Quantitation of phosphorylation signals in U87 cells with stable PTN/ALK double knockdown, which abolished the growth of SC tumor xenografts (PTN Rz66/ALK Rz12-1, gray bars), compared with control cells (black bars). (B) Representative examples of various film exposures with (upper panels) a total overview and (lower panels) selected areas after shorter or longer exposure time. (C) The selected double knockdown cell line shows markedly reduced tumor growth compared with control cells also in an orthotopic tumor model.

more efficient especially in long-term therapy. In fact, previous studies on PTN or ALK single knockdown showed best results only on the selection of stable cell clones with highest knockdown efficacies [21,25]. This is barely achievable and thus probably not realistic in the setting of a therapeutic intervention *in vivo*. Moreover, the existence of an alternative ligand for the ALK receptor, MK [38], may limit the therapeutic efficacy of a single knockdown of PTN. Thus, this study aimed at the parallel knockdown of both ligand and receptor of the PTN signal transduction pathway.

Selection of Target Molecules for Double Knockdown

Besides PTN, we selected ALK because this receptor tyrosine kinase has been shown to act as a PTN binding molecule and thus as a direct receptor [24,39] as well as to be a crucial downstream signal transduction molecule in the RPTPβ/ζ pathway on PTN activation [31]. Hence, despite one study that failed to show the activation of ALK by PTN [40], a huge body of evidence indicates that ALK is crucial in PTN signal transduction. Consequently, the issue whether both pathways, RPTPβ/ζ–dependent and –independent, exist in parallel and are functionally relevant for PTN signaling, is less important here about the expected increase in therapeutic efficacy on double knockdown of PTN and ALK. This is also true for the distinction between the two naturally occurring forms of PTN (15 and 18 kDa) [39]. PTN 15 and PTN 18 have been described to act differently, with PTN 15 promoting glioblastoma proliferation in an ALK-dependent fashion and immobilized PTN 18 promoting haptotactic migration of glioblastoma cells in an RPTPβ/ζ–dependent fashion [39]. However, because the PTN isoforms differ by posttranslational processing of 12 C-terminal amino acids, they are both targeted in our approach.

Indeed, the parallel knockdown of PTN and ALK strongly enhanced antitumorigenic effects in glioblastoma growth as shown here in different cell lines and in different *in vitro* and *in vivo* models. Our expression analysis data, however, also demonstrate striking differences between various glioblastoma cell lines regarding PTN,

ALK, MK, and RPTPβ/ζ expression, which is in agreement and further extends previous studies [25,39,41]. This is true, for example, regarding the absence of ALK and RPTPβ/ζ in T98G cells, and consequently, ribozyme-mediated ALK targeting did not exert any growth-inhibitory effects in this cell line (data not shown). Because PTN knockdown, however, still provides antitumorigenic effects in T98G cells (data not shown), this also indicates that non–ALK-mediated PTN signal transduction pathways exist as suggested previously (see, e.g., [40]).

Impact of PTN/ALK Targeting on Signal Transduction

Our phosphorylation assay data also demonstrate the presence of PTN/ALK–dependent pathways, beyond the ones already described in the literature, initiating proliferation and tumorigenesis. More specifically, it was shown previously that PTN activates phosphatidylinositol 3-kinase and MAPK pathways [24,25] and induces the phosphorylation of ALK and of the downstream effector molecules IRS-1, Shc, phospholipase C-γ, and phosphatidylinositol 3-kinase, thus mediating growth stimulatory [24] and antiapoptotic effects [23]. Furthermore, ribozyme-mediated targeting of ALK prevented PTN-stimulated Akt phosphorylation, leading to antitumorigenic effects [25]. Importantly, the stable down-regulation used here, as opposed to transient targeting or stimulation approaches, relies on a somewhat prolonged cultivation of the cells under knockdown conditions and thus allowed us to study the cells after adaptation, i.e., after at least partial counterregulation of growth inhibitory effects, thus mimicking prolonged therapeutic intervention. Interestingly, the inhibition of the ERK1/2 signaling pathway, which has been described previously to be relevant in PTN and ALK [38–40,42–44] signaling, was lost on prolonged double knockdown of PTN and ALK, as indicated by unchanged degrees of phosphorylation. This suggests the parallel activation of other proliferative pathways that signal through ERK1/2. In this context, it should be noted that Heroult et al. [45] found PTN to associate with VEGF165 through the thrombospondin type I repeat domains, suggesting that PTN blocks VEGF165 binding to its receptor. Consequently, this effect would be abrogated on PTN targeting and may account for unchanged net levels of ERK1/2. In fact, the constitutive activation of MAPK particularly in U87 glioblastoma cells has also been described previously [25].

Strikingly, the PTN/ALK double knockdown is sufficient to induce the complete abolishment of tumor growth as in the case of Rz66/12-1, also indicating that pathways other than ERK1/2 determine the (loss of) tumorigenic potential of glioblastoma cells. Indeed, the phosphorylation array shows significant changes in the activation of other downstream signal transduction molecules, which persist also for a prolonged knockdown period. This is true for Akt3 and, to a minor extent, for Akt2, which is in agreement with earlier reports that Akt acts downstream of ALK [38] and is stimulated by PTN in ALK-expressing but not in ALK-negative cell lines [23,25,39]. Because the serine/threonine kinases Akt (also called PKB) are known to be regulators of growth factor–mediated cell signaling involved in various biologic processes including cell proliferation and tumorigenesis, the finding of Akt inactivation on double knockdown fits well to the observed antitumorigenic phenotype.

Identification of Other Pathways Relevant in PTN/ALK Signaling

Other pathways that have been less well explored or so far have not been described at all in the context of PTN/ALK seem to be involved as well. The antibody array data indicate a marked activation of GSK3α and GSK3β, which are involved in the regulation of various cell functions, on double knockdown of PTN and ALK. This is in line with the above-mentioned finding of decreased Akt activity on ribozyme transfection, because PKB/Akt, which is frequently activated in cancers [46], phosphorylates and inhibits GSK3, with decreased Akt activity, consequently leading to GSK3 activation. Furthermore, certain growth factors including, for example, endothelial growth factor, have been shown to inhibit GSK3 activity (see [47]), and our results now extend these findings toward PTN/ALK. The activation of GSK3 on PTN/ALK knockdown is particularly important because GSK3 acts as a potential tumor suppressor protein in the Wnt signaling pathway, thus leading to decreased expression of oncogenic proteins (see [48] for review), and the reversal of the aberrant GSK3 inhibition in glioblastoma cells may well contribute to the reduced tumorigenesis observed in our study.

Likewise, a marked activation of p38 is observed on PTN/ALK double knockout. Because the p38 MAPK pathway has been described as a negative regulator of cell proliferation and tumorigenesis with persistent activation of the p38 pathway, thus inhibiting tumor formation, this finding again fits very well to the observed antitumorigenic effects on ribozyme-mediated double targeting of PTN and ALK.

Mad1 is a substrate of both p90 RSK and p70 S6 kinase, and the phosphorylation of Mad1 accelerates its ubiquitination and proteasome-mediated degradation, thereby inhibiting its tumor suppressor function [49]. Consequently, because the phosphorylation and thus activation of RSK promotes tumor cell proliferation, the absence of activated RSK2 on PTN/ALK double knockdown again corresponds to the finding of decreased proliferation. In contrast, however, the activation rather than inactivation of P70S6 and RSK1 kinases may at least partially counteract this effect by restoring Mad1 degradation and stimulation of cell proliferation under double targeting conditions. This indicates an obviously more complex interplay between both pathways acting on Mad1 and thus on tumor cell proliferation, which will require further analysis also in the context of PTN/ALK double knockdown.

Finally, the double knockdown of PTN/ALK led to the inactivation of Hsp27. Heat shock proteins including Hsp27, which are induced in cells exposed to stress and which function as molecular chaperons in protein folding, have been implicated in cancer [50], and Hsp27 is involved in cell growth. Consistent with that, Hsp27 expression has been shown to correlate with the degree of malignancy of glial tumors with very high levels in glioblastomas (WHO grade IV) as well as in U87 cells [51]. Again, the reduction of activated Hsp27 below the level of detection on ALK/PTN double knockdown may add to the antiproliferative effects of the ribozymes.

Thus, beyond the already established signal transduction pathways for PTN and ALK, we identify other relevant pathways, indicating a more complex pattern of PTN-mediated signaling through ALK.

Therapeutic Relevance of Double Inhibition Strategies

In recent years, gene targeting approaches have gained increased attention owing to the discovery and exploration of RNAi *in vitro* and particularly *in vivo* (see, e.g., [52] for review), with siRNA probably providing even more powerful tools than ribozymes especially for the transient therapeutic knockdown. As shown in this study, the establishment of double targeting strategies, which go beyond the knockdown of a single gene product such as PTN [22] and may also include alternative strategies including inhibitory antibodies

for ALK [40], will likely enhance therapeutic efficacies. This may be because the inhibition of PTN or ALK is less than 100%, which would probably also be true in any therapeutic setting and suggests that additive effects are observed on double knockdown. Furthermore, it has been shown in other systems that the independent inhibition of a given pathway at two steps can exert synergistic effects, e.g., by helping to avoid autocrine counterregulation events or the formation of resistance. This may be true here particularly in the light of the complexity of the pathway(s) about the existence of two ligands and two receptors. Thus, double knockdown strategies may offer novel approaches for therapeutic interventions, particularly in malignancies with poor prognosis as, for example, in glioblastoma.

Acknowledgments

The authors thank Fatma Aktuna, Olga Häckel, Julia Hagenbusch, Helga Radler, and Andrea Wüstenhagen for their expert help with the experiments, Thomas Büch for helpful discussions, and Marc Vigny for providing the PTN antibody.

References

[1] Holland EC (2000). Glioblastoma multiforme: the terminator. *Proc Natl Acad Sci USA* **97** (12), 6242–6244.

[2] Zhang N, Zhong R, Wang ZY, and Deuel TF (1997). Human breast cancer growth inhibited *in vivo* by a dominant negative pleiotrophin mutant. *J Biol Chem* **272**, 16733–16736.

[3] Aigner A, Brachmann P, Beyer J, Jager R, Raulais D, Vigny M, Neubauer A, Heidenreich A, Weinknecht S, Czubayko F, et al. (2003). Marked increase of the growth factors pleiotrophin and fibroblast growth factor-2 in serum of testicular cancer patients. *Ann Oncol* **14** (10), 1525–1529.

[4] Jager R, Noll K, Havemann K, Pfluger KH, Knabbe C, Rauvala H, and Zugmaier G (1997). Differential expression and biological activity of the heparin-binding growth-associated molecule (HB-GAM) in lung cancer cell lines. *Int J Cancer* **73** (4), 537–543.

[5] Czubayko F, Schulte AM, Berchem GJ, and Wellstein A (1996). Melanoma angiogenesis and metastasis modulated by ribozyme targeting of the secreted growth factor pleiotrophin. *Proc Natl Acad Sci USA* **93**, 14753–14758.

[6] Mailleux P, Vanderwinden JM, and Vanderhaeghen JJ (1992). The new growth factor pleiotrophin (HB-GAM) mRNA is selectively present in the meningothelial cells of human meningiomas. *Neurosci Lett* **142**, 31–35.

[7] Fang WJ, Hartmann N, Chow D, Riegel AT, and Wellstein A (1992). Pleiotrophin stimulates fibroblasts, endothelial and epithelial cells, and is expressed in human cancer. *J Biol Chem* **267**, 25889–25897.

[8] Klomp HJ, Zernial O, Flachmann S, Wellstein A, and Juhl H (2002). Significance of the expression of the growth factor pleiotrophin in pancreatic cancer patients. *Clin Cancer Res* **8** (3), 823–827.

[9] Schulte AM, Lai S, Kurtz A, Czubayko F, Riegel AT, and Wellstein A (1996). Human trophoblast and choriocarcinoma expression of the growth factor pleiotrophin attributable to germ line insertion of an endogenous retrovirus. *Proc Natl Acad Sci USA* **93**, 14759–14764.

[10] Nakagawara A, Milbrandt J, Muramatsu T, Deuel TF, Zhao H, Cnaan A, and Brodeur GM (1995). Differential expression of pleiotrophin and midkine in advanced neuroblastoma. *Cancer Res* **55**, 1792–1797.

[11] Muller S, Kunkel P, Lamszus K, Ulbricht U, Lorente GA, Nelson AM, von Schack D, Chin DJ, Lohr SC, Westphal M, et al. (2003). A role for receptor tyrosine phosphatase zeta in glioma cell migration. *Oncogene* **22** (43), 6661–6668.

[12] Ulbricht U, Brockmann MA, Aigner A, Eckerich C, Muller S, Fillbrandt R, Westphal M, and Lamszus K (2003). Expression and function of the receptor protein tyrosine phosphatase zeta and its ligand pleiotrophin in human astrocytomas. *J Neuropathol Exp Neurol* **62** (12), 1265–1275.

[13] Mentlein R and Held-Feindt J (2002). Pleiotrophin, an angiogenic and mitogenic growth factor, is expressed in human gliomas. *J Neurochem* **83** (4), 747–753.

[14] Czubayko F, Riegel AT, and Wellstein A (1994). Ribozyme-targeting elucidates a direct role of pleiotrophin in tumor growth. *J Biol Chem* **269**, 21358–21363.

[15] Choudhuri R, Zhang HT, Donnini S, Ziche M, and Bicknell R (1997). An angiogenic role for the neurokines midkine and pleiotrophin in tumorigenesis. *Cancer Res* **57**, 1814–1819.

[16] Courty J, Dauchel MC, Caruelle D, Perderiset M, and Barritault D (1991). Mitogenic properties of a new endothelial cell growth factor related to pleiotrophin. *Biochem Biophys Res Commun* **180**, 145–151.

[17] Rauvala H (1989). An 18-kd heparin-binding protein of developing brain that is distinct from fibroblast growth factors. *EMBO J* **8**, 2933–2941.

[18] Li YS, Milner PG, Chauhan AK, Watson MA, Hoffman RM, Kodner CM, Milbrandt J, and Deuel TF (1990). Cloning and expression of a developmentally regulated protein that induces mitogenic and neurite outgrowth activity. *Science* **250**, 1690–1694.

[19] Weber D, Klomp HJ, Czubayko F, Wellstein A, and Juhl H (2000). Pleiotrophin can be rate-limiting for pancreatic cancer cell growth. *Cancer Res* **60** (18), 5284–5288.

[20] Satyamoorthy K, Oka M, and Herlyn M (2000). An antisense strategy for inhibition of human melanoma growth targets the growth factor pleiotrophin. *Pigment Cell Res* **13** (Suppl 8), 87–93.

[21] Grzelinski M, Bader N, Czubayko F, and Aigner A (2005). Ribozyme-targeting reveals the rate-limiting role of pleiotrophin in glioblastoma. *Int J Cancer* **117**, 942–951.

[22] Grzelinski M, Urban-Klein B, Martens T, Lamszus K, Bakowsky U, Hobel S, Czubayko F, and Aigner A (2006). RNA interference–mediated gene silencing of pleiotrophin through polyethylenimine-complexed small interfering RNAs *in vivo* exerts antitumoral effects in glioblastoma xenografts. *Hum Gene Ther* **17** (7), 751–766.

[23] Bowden ET, Stoica GE, and Wellstein A (2002). Anti-apoptotic signaling of pleiotrophin through its receptor, anaplastic lymphoma kinase. *J Biol Chem* **277** (39), 35862–35868.

[24] Stoica GE, Kuo A, Aigner A, Sunitha I, Souttou B, Malerczyk C, Caughey DJ, Wen D, Karavanov A, Riegel AT, et al. (2001). Identification of anaplastic lymphoma kinase as a receptor for the growth factor pleiotrophin. *J Biol Chem* **276** (20), 16772–16779.

[25] Powers C, Aigner A, Stoica GE, McDonnell K, and Wellstein A (2002). Pleiotrophin signaling through anaplastic lymphoma kinase is rate-limiting for glioblastoma growth. *J Biol Chem* **277** (16), 14153–14158.

[26] Le Beau MM, Bitter MA, Larson RA, Doane LA, Ellis ED, Franklin WA, Rubin CM, Kadin ME, and Vardiman JW (1989). The t(2;5)(p23;q35): a recurring chromosomal abnormality in Ki-1–positive anaplastic large cell lymphoma. *Leukemia* **3** (12), 866–870.

[27] Mason DY, Bastard C, Rimokh R, Dastugue N, Huret JL, Kristoffersson U, Magaud JP, Nezelof C, Tilly H, Vannier JP, et al. (1990). CD30-positive large cell lymphomas ("Ki-1 lymphoma") are associated with a chromosomal translocation involving 5q35. *Br J Haematol* **74** (2), 161–168.

[28] Morris SW, Kirstein MN, Valentine MB, Dittmer KG, Shapiro DN, Saltman DL, and Look AT (1994). Fusion of a kinase gene, *ALK*, to a nucleolar protein gene, *NPM*, in non–Hodgkin's lymphoma. *Science* **263** (5151), 1281–1284.

[29] Pulford K, Morris SW, and Turturro F (2004). Anaplastic lymphoma kinase proteins in growth control and cancer. *J Cell Physiol* **199** (3), 330–358.

[30] Meng K, Rodriguez-Pena A, Dimitrov T, Chen W, Yamin M, Noda M, and Deuel TF (2000). Pleiotrophin signals increased tyrosine phosphorylation of beta beta-catenin through inactivation of the intrinsic catalytic activity of the receptor-type protein tyrosine phosphatase beta/zeta. *Proc Natl Acad Sci USA* **97** (6), 2603–2608.

[31] Perez-Pinera P, Zhang W, Chang Y, Vega JA, and Deuel TF (2007). Anaplastic lymphoma kinase is activated through the pleiotrophin/receptor protein–tyrosine phosphatase beta/zeta signaling pathway: an alternative mechanism of receptor tyrosine kinase activation. *J Biol Chem* **282** (39), 28683–28690.

[32] Ulbricht U, Eckerich C, Fillbrandt R, Westphal M, and Lamszus K (2006). RNA interference targeting protein tyrosine phosphatase zeta/receptor-type protein tyrosine phosphatase beta suppresses glioblastoma growth *in vitro* and *in vivo*. *J Neurochem* **98** (5), 1497–1506.

[33] Kunkel P, Ulbricht U, Bohlen P, Brockmann MA, Fillbrandt R, Stavrou D, Westphal M, and Lamszus K (2001). Inhibition of glioma angiogenesis and growth *in vivo* by systemic treatment with a monoclonal antibody against vascular endothelial growth factor receptor-2. *Cancer Res* **61** (18), 6624–6628.

[34] Abuharbeid S, Apel J, Sander M, Fiedler B, Langer M, Zuzarte ML, Czubayko F, and Aigner A (2004). Cytotoxicity of the novel anti-cancer drug rViscumin depends on HER-2 levels in SKOV-3 cells. *Biochem Biophys Res Commun* **321** (2), 403–412.

[35] Wellstein A, Lupu R, Zugmaier G, Flamm SL, Cheville AL, Delli Bovi P, Basilico C, Lippman ME, and Kern FG (1990). Autocrine growth stimulation by secreted Kaposi's fibroblast growth factor but not by endogenous basic fibroblast growth factor. *Cell Growth Differ* **1**, 63–71.

[36] Liang CC, Park AY, and Guan JL (2007). *In vitro* scratch assay: a convenient and inexpensive method for analysis of cell migration *in vitro*. *Nat Protoc* **2** (2), 329–333.

[37] Muramatsu T (2002). Midkine and pleiotrophin: two related proteins involved in development, survival, inflammation and tumorigenesis. *J Biochem (Tokyo)* **132** (3), 359–371.

[38] Stoica GE, Kuo A, Powers C, Bowden ET, Sale EB, Riegel AT, and Wellstein A (2002). Midkine binds to anaplastic lymphoma kinase (ALK) and acts as a growth factor for different cell types. *J Biol Chem* **277** (39), 35990–35998.

[39] Lu KV, Jong KA, Kim GY, Singh J, Dia EQ, Yoshimoto K, Wang MY, Cloughesy TF, Nelson SF, and Mischel PS (2005). Differential induction of glioblastoma migration and growth by two forms of pleiotrophin. *J Biol Chem* **280** (29), 26953–26964.

[40] Moog-Lutz C, Degoutin J, Gouzi JY, Frobert Y, Brunet-de Carvalho N, Bureau J, Creminon C, and Vigny M (2005). Activation and inhibition of anaplastic lymphoma kinase receptor tyrosine kinase by monoclonal antibodies and absence of agonist activity of pleiotrophin. *J Biol Chem* **280** (28), 26039–26048.

[41] Brockmann MA, Ulbricht U, Gruner K, Fillbrandt R, Westphal M, and Lamszus K (2003). Glioblastoma and cerebral microvascular endothelial cell migration in response to tumor-associated growth factors. *Neurosurgery* **52** (6), 1391–1399; discussion 1399.

[42] Deuel TF, Zhang N, Yeh HJ, Silos-Santiago I, and Wang ZY (2002). Pleiotrophin: a cytokine with diverse functions and a novel signaling pathway. *Arch Biochem Biophys* **397** (2), 162–171.

[43] Degoutin J, Vigny M, and Gouzi JY (2007). ALK activation induces Shc and FRS2 recruitment: signaling and phenotypic outcomes in PC12 cells differentiation. *FEBS Lett* **581** (4), 727–734.

[44] Souttou B, Carvalho NB, Raulais D, and Vigny M (2001). Activation of anaplastic lymphoma kinase receptor tyrosine kinase induces neuronal differentiation through the mitogen-activated protein kinase pathway. *J Biol Chem* **276** (12), 9526–9531.

[45] Heroult M, Bernard-Pierrot I, Delbe J, Hamma-Kourbali Y, Katsoris P, Barritault D, Papadimitriou E, Plouet J, and Courty J (2004). Heparin affin regulatory peptide binds to vascular endothelial growth factor (VEGF) and inhibits VEGF-induced angiogenesis. *Oncogene* **23** (9), 1745–1753.

[46] Samuels Y and Ericson K (2006). Oncogenic PI3K and its role in cancer. *Curr Opin Oncol* **18** (1), 77–82.

[47] Cohen P and Frame S (2001). The renaissance of GSK3. *Nat Rev Mol Cell Biol* **2** (10), 769–776.

[48] Jope RS, Yuskaitis CJ, and Beurel E (2007). Glycogen synthase kinase-3 (GSK3): inflammation, diseases, and therapeutics. *Neurochem Res* **32** (4–5), 577–595.

[49] Zhu J, Blenis J, and Yuan J (2008). Activation of PI3K/Akt and MAPK pathways regulates Myc-mediated transcription by phosphorylating and promoting the degradation of Mad1. *Proc Natl Acad Sci USA* **105** (18), 6584–6589.

[50] Sarto C, Binz PA, and Mocarelli P (2000). Heat shock proteins in human cancer. *Electrophoresis* **21** (6), 1218–1226.

[51] Zhang R, Tremblay TL, McDermid A, Thibault P, and Stanimirovic D (2003). Identification of differentially expressed proteins in human glioblastoma cell lines and tumors. *Glia* **42** (2), 194–208.

[52] Aigner A (2007). Applications of RNA interference: current state and prospects for siRNA-based strategies *in vivo*. *Appl Microbiol Biotechnol* **76** (1), 9–21.